# A NEURON MODEL WITH SPATIALLY DISTRIBUTED SYNAPTIC INPUT

RUSSELL D. FERNALD

*From the Department of Biomedical Engineering and The Johnson Research Foundation, University of Pennsylvania, Philadelphia, Pennsylvania 19104. Dr. Fernald's present address is the Max Planck Institute for Psychiatry, 8 München 23, West Germany.*

ABSTRACT I have assembled a neuron model simulating contiguous patches of nerve cell membrane. With this model I have examined the functional significance of different spatial and temporal distributions of synaptic inputs. The model consists of two terminal electronic analogue circuits with inputs controlled by a LINC computer. One terminal represents the inside of a membrane patch, the other represents the outside. Two circuit designs are used: one simulates spike-generating regions of the neuron, the other simulates subthreshold activity in inexcitable regions. To simulate a neuron, patches are assembled in various spatial arrangements by suitable connection to the "intracellular" nodes. Thus the relation of neuron geometry to aspects of spatiotemporal summation of synaptic inputs can be investigated readily. Performance of the model is assessed by comparison with results from microelectrode studies in the cochlear nucleus of the cat. In particular, the peristimulus time (PST) histogram and averaged membrane potential are used for quantitative comparison. The model suggests that the geometry of the neuron's receptive surface can account for a wide variety of physiologically observed behavior, particularly in response to dynamic stimuli.

## INTRODUCTION

Information processing by assemblies of neurons depends on the detailed properties of individual cells as well as on interconnections between cells. As more sophisticated experiments describe the behavior of nervous systems in greater detail, models of that behavior must include closer approximations both of the neuron itself and of neural interconnections. In particular, it is necessary in modeling studies to evaluate the functional significance of different spatial distributions of synaptic inputs. There is ample physiological evidence suggesting that it is an oversimplification to represent the synaptic input to a neuron as occurring at a single point. The branched dendritic receptive surface area can be many times larger than that of the cell body (Rall, 1961/1962) and can modify readily the state of the membrane potential (Rall, 1964; Rall, et al., 1967).

I have assembled a neuron model which simulates contiguous patches on a nerve cell membrane. With this model synaptic inputs may be placed at an arbitrary location on the equivalent neuronal surface with respect to the site of spike initiation.

This model has been used successfully to simulate results from microelectrode studies of single neurons in cat cochlear nucleus. The model has also predicted some neuronal behavior which subsequent physiological experiments have verified. Finally, the model suggests a possible mechanism for achieving sensitivity to the direction of change of a dynamically varying stimulus in neurons of the sensory pathways.

## EXPERIMENTAL BACKGROUND

Recordings, both extracellular and intracellular, have been made from neurons of the cat cochlear nucleus during presentation of frequency modulated tonal stimulus. Details of the experimental procedure are reported elsewhere (Erulkar et al., 1968; Fernald, 1968; Fernald and Gerstein, 1970;[1] Gerstein et al., 1968). Three main results from these studies are pertinent here: first, three types of spike firing patterns result from frequency modulated acoustic stimuli; second, the over-all shape of the firing pattern remains nearly constant over a range of frequency modulation rates; third, the excursions of the membrane potential do not necessarily predict the spike firing pattern.

The three different types of firing patterns are classified according to their symmetry with regard to increasing or decreasing frequency of the stimulus (see Fig. 1). (The frequency modulated stimuli used in this study were all symmetrical with respect to a point in time; the symmetries of the responses are given with respect to the same point in time). In Fig. 1 (top), unit CN 62-2 has "mirror symmetry" around the central coordinate which corresponds to the highest stimulus frequency. For this class of neurons the spike response is approximately equal to a given stimulus frequency, whether in the ascending or descending portion of the stimulus. The second class responses may be characterized as "translation symmetry" with respect to the central coordinate (unit CN 53-7, Fig. 1, middle). Such neurons show approximately the same response pattern to the stimulus whether it is of increasing or decreasing frequency. There is no dependence of the response pattern on exact stimulus frequency or sequence of presentation. The third class of neurons (unit CN 58-5, Fig. 1, bottom) has a response pattern which is asymmetric with respect to the central coordinate. For this class of neurons the response depends not only on the stimulus frequency, but also on the direction of change of that frequency.

A second main experimental result was that the shape of the spike firing patterns remained constant over a range of frequency modulation rates. Fig. 2 shows the

[1] Fernald, R. D., and G. L. Gerstein. 1970. To be published.

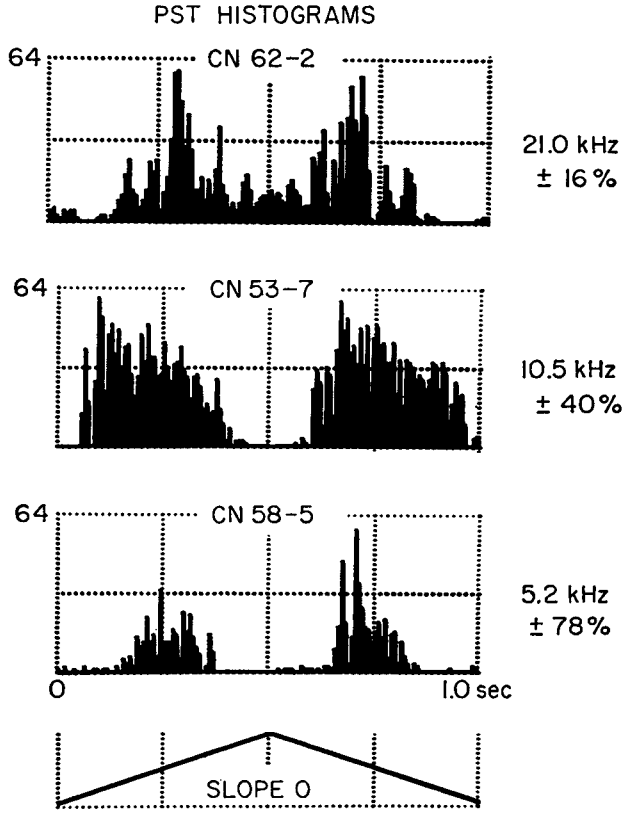




FIGURE 1 PST histograms of firing patterns for three different neurons in the cat cochlear nucleus in response to frequency modulated tones. The three classes of symmetry with respect to the instant at which the lowest frequency is presented are: top, mirror symmetry (number of stimuli = 29); middle, translation symmetry ($S$ = 28); and bottom, asymmetry ($S$ = 31).

firing patterns for a neuron in the cochlear nucleus under stimulation at three different frequency modulation rates. To facilitate comparison, the spike firing histograms are compiled only during the times when the stimulus frequencies are changing (note time scales). The stimuli in these experiments were tones modulated by trapezoidal wave forms to allow various rates of change of frequency independent of the stimulus repetition rate (see Erulkar et al., 1968, Figs. 4 and 5).

The important feature of these three histograms is their common shape. Although the change of stimulus frequency with respect to time ($df/dt$) increases threefold, the firing patterns remain invariant. This shape invariance as a function of $df/dt$ has been found in all neurons studied in cochlear nucleus (Erulkar et al., 1968). Thus, these neurons have a response pattern which is not sensitive to changes in the magnitude $df/dt$ except through trivial compression along the time axis.

A third result of experimental studies of cochlear nucleus neurons was that the

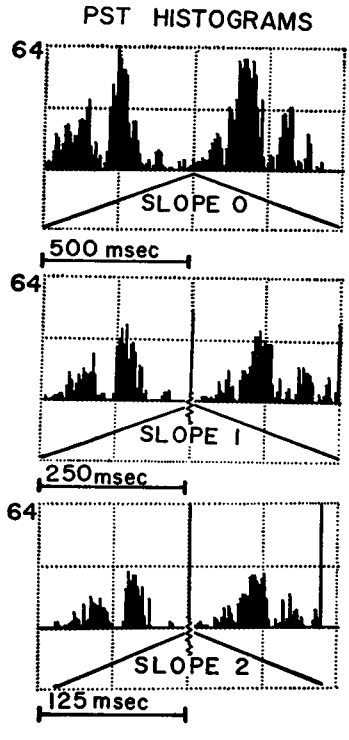


FIGURE 2 Three PST histograms from one cell in response to three rates of frequency modulation. (Note the different time scales.)

measured intracellular potential did not necessarily reflect the spike firing pattern (Gerstein et al., 1968; Starr and Britt, 1970). The measured membrane potential in several cases showed an excursion above the apparent spike threshold without concomitant spike firings.

Anatomically, the cochlear nucleus has three main subdivisions: posteroventral (PVCN), anteroventral (AVCN), and dorsal (DCN) (Rose et al., 1959), although Lorente de No (1933) reported projections from cochlear nerve into 13 identifiable subdivisions. Ramon-Moliner (1968) describes cell types in the major divisions of the cochlear nucleus according to their dendritic morphology (p. 260): "The cells of the ventral cochlear nucleus are characterized by round cell bodies and a few dendritic trunks, not too long, that immediately subdivide into rich ramifications. The details of these ramifications vary according to the particular region of the cochlear complex." Besides the normal afferent fiber input to the ventral cochlear nucleus (VCN), there are the clawlike calyces of Held which always make axosomatic contact (Ramon-Moliner, 1968). The dendrites of VCN cells are classified in his system as "extremely tufted" in common with dendritic types from several other sensory relays. The cells in the dorsal cochlear nucleus have fairly long

"wavy" dendrites with a bipolar orientation (Ramon-Moliner, 1968). This phylogenetically more recent portion of the cochlear nucleus also appears to have substantially different response properties (Molnar and Pfeiffer, 1968). Thus for cells in the cochlear nucleus the dendritic structure can be expected to be an important factor in determining the responses of the neuron.

## PREVIOUS MODELS OF DENDRITIC TREES

Rall (1961, 1962, 1964) has presented a general model for dendritic trees consisting of a series of discrete compartments. Spatial nonuniformity is represented by differences between compartments. Using differential equations to describe the cell membrane in each compartment, Rall has applied the model to a variety of situations. One application of particular interest here is the effect of different spatiotemporal input sequences on transient soma depolarization. Using a 10-compartment model in which the first compartment represented the soma, and the second through tenth compartments, successively more remote dendritic surfaces, Rall examined two excitatory input pulse sequences (Rall, 1964, Fig. 7): one moving toward the soma and one moving away from the soma. The differences in soma potential are striking. Sweeping toward the soma results in a large potential with a long latency and rapid decay time. Sweeping away from the soma, on the other hand, gives a more rapid rise to a lower level which has a slower decay. The effect of distributing the same excitation uniformly over the same compartments at a single time gives an intermediate effect. Clearly, depending on the threshold and state of excitation in the soma, the spike firings of the cell could be quite different for the two cases. In his work, however, Rall has considered only subthreshold behavior. The ways such subthreshold phenomena might influence spike firings have not been modeled in any detail.

In the cochlear nucleus various electrophysiological findings may in general be explained by a distribution of synaptic input over the surface of the neuron being studied (Erulkar et al., 1968; Gerstein et al., 1968; Starr and Britt, 1970). Anatomical descriptions support the idea that some cells in the cochlear nucleus have a large dendritic surface area (Ramon-Moliner, 1962, 1968). To attempt a systematic explanation of the potential role of dendritic inputs to cells in the cochlear nucleus, the following model was assembled.

## THE MODEL

### *Simulation of a Membrane Patch*

To simulate a distributed denditic surface coupled to an active, spike-initiating somatic surface, I have used nonlinear analogue circuits developed by E. R. Lewis (1964, 1965, 1968). The two-terminal electronic circuit is designed to represent a patch of nerve cell membrane 1 $cm^2$ in area. Two realizations have been used: one to simulate active or electrically excitable membrane (spike initiator patch), the second to simulate passive, subthreshold membrane (subthreshold patch). The circuit for subthreshold events is valid for the graded be-

havior of EPSP (excitatory postsynaptic potential) and IPSP (inhibitory postsynaptic potential) synaptic input, but is incapable of large excursions of membrane potential such as spikes.

Between the two terminals of each circuit are six parallel networks. Four are approximate realizations of the elements specified by Hodgkin and Huxley: membrane capacitance, leakage current, sodium current, and potassium current. Two are approximate realizations of synaptic conductances: inhibitory and excitatory.

The electrical properties of the circuits are quite similar to those measured in physiological preparations. The spike is clipped at 0 v, but otherwise exhibits a time course quite similar to spikes physiologically observed (Fernald, 1967, 1968). There is a threshold, absolute and relative refractory periods, and a postspike hyperpolarization.

### *Simulation of Synaptic Input*

Since these models are two terminal networks, the input and output terminals are equivalent. Synaptic currents require the presence of a chemical transmitter substance which is presumed independent of the intracellular potential. Thus simulation of a synaptic current requires a third terminal which allows independent input of simulated transmitter substance. Two such terminals are provided in the models; one for excitatory synaptic inputs and one for inhibitory synaptic inputs.

The inhibitory synaptic circuit produces a hyperpolarizing current proportional to input voltage and approaches zero as the simulated membrane potential approaches $-8$ v (corresponding to $-80$ mv in a nerve cell). The inhibitory synaptic current is unable to hyperpolarize the simulated membrane potential beyond this level. This is in general agreement with findings in nerve cells.

The excitatory synaptic input similarly produces a depolarizing current proportional to input voltage which approaches zero as the membrane potential approaches zero. In neurons, the excitatory synapse is usually considered to change transiently the local permeability of the postsynaptic membrane to all ions. Thus the nerve synapse becomes ineffective when the postsynaptic membrane potential reaches the equilibrium potential of 0 mv. In most cases the range of interesting behavior for the membrane potential is below the threshold of spike initiation (about $-50$ mv). Once the threshold has been exceeded, regenerative permeability changes and initiation of an action potential occur, so that EPSP activity is of little consequence until the firing is completed. For these reasons the excitatory synaptic circuit is an adequate model for this work.

Since it is assumed that synaptic activity reflects local conductance changes, the size and hence the effectiveness of any PSP depends on the local PSP. For small excursions of the membrane potential, however, local conductance changes can be closely approximated by membrane potential changes as in the model presented here.

### *Assemblies of Circuits*

Several circuits can be used to represent a single neuron by appropriately connecting their intracellular nodes (Fig. 3). The nodes representing the outside of the membrane patches are connected together since the extracellular fluid impedance is assumed negligible compared to the intracellular fluid impedance. Such an assembly approximates a spatial distribution of nerve cell membrane in a manner analogous to the compartment array of Rall (1964). A salient difference, however, is the connection of patches capable of graded subthreshold response to "active" patches which can initiate classic action potentials (spikes). Spikes

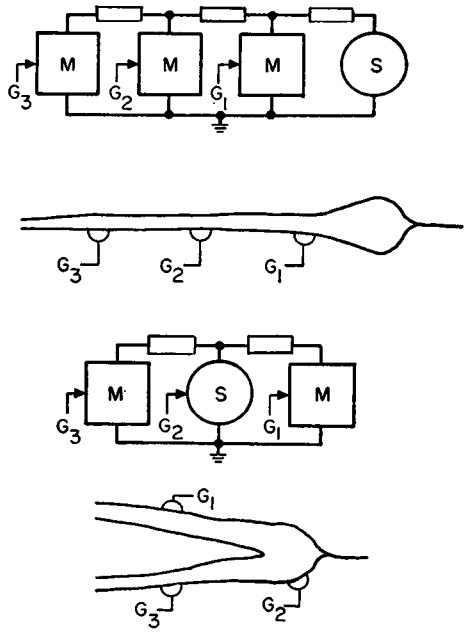


FIGURE 3 Two arrays of circuits representing neurons with spatially distributed inputs.

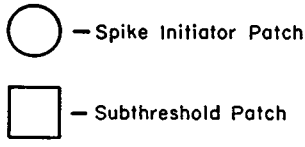


elicited in the model spread electrotonically back into the subthreshold patches, just as in real neurons the spikes spread back into dendritic structures.

### *Control of Inputs to the Model*

The inputs to the neuron model are controlled by a computer program. The same program has a provision to compute simultaneously appropriate spike histograms. As shown in the system block diagram (Fig. 4), the LINC computer, under program control, delivers a 12 bit word to an external buffer register. Each bit or bit change is available either to trigger an external pulse generator directly or to gate an externally generated train of pulses, which can be periodic or random. These gated signals are fed into the synaptic terminals of the model through an RC pulse-shaping circuit to effect a closer approximation of the physiologically observed PSP (Fernald, 1968). The output membrane potential of the spike initiator patch of interest goes to a discriminator which is set to deliver a standard LINC pulse to the computer for each spike firing. The control program uses this pulse to compute the spike firing histograms (Gerstein and Kiang, 1960). The membrane potential from each of the assembled patches is also tape-recorded (FM).

For any given signal line, the onset time and duration of several gates within the main

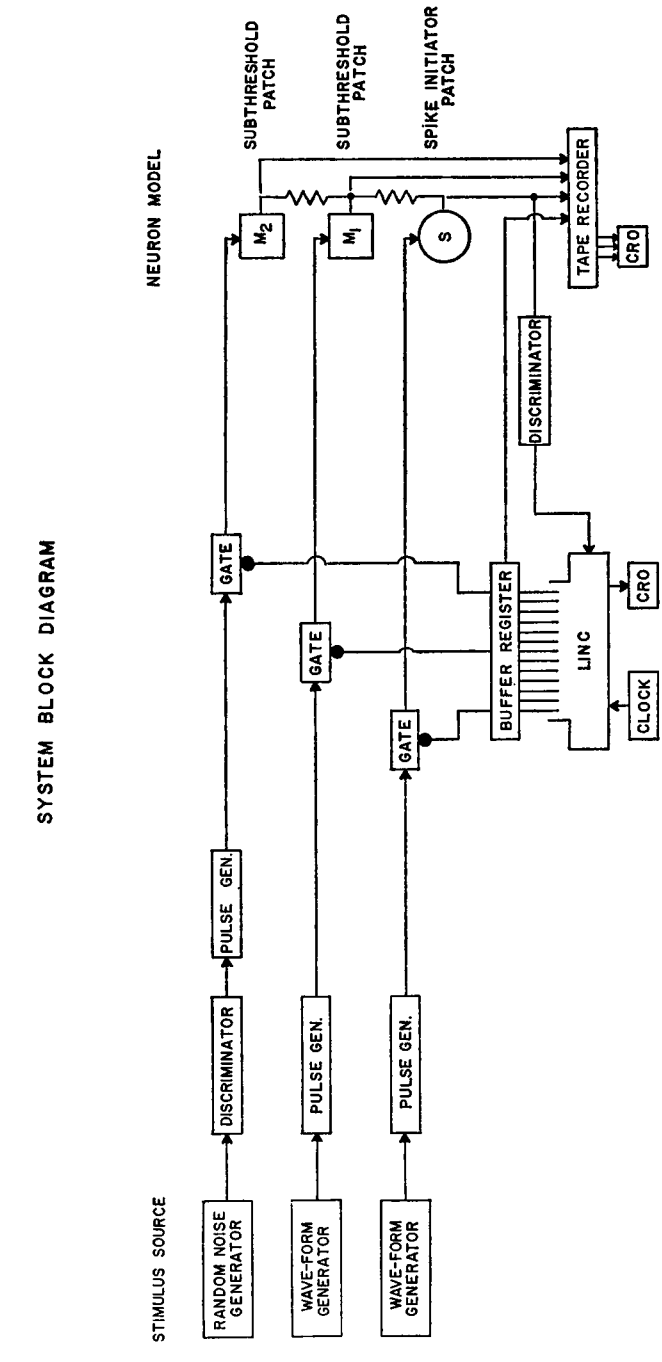


FIGURE 4 Block diagram of system used to control the neuron model.

stimulus cycle can be chosen. The input pulses to the model are generated by a Tektronix type 161 pulse generator (Tektronix, Inc., Beaverton, Ore.). To give a train of pulses a Tektronix wave-form generator, type 162, is used to trigger the pulse generator, and the output is then gated as described above.

Another available stimulus condition consists of random pulses (indicated in the figures by *N*). This "pulse noise input" was always a Poisson pulse train.

### *Input Sequence*

A variety of stimuli for the model were chosen, taking into account the known behavior of primary auditory fibers which terminate on cochlear nucleus cells. Extensive data about

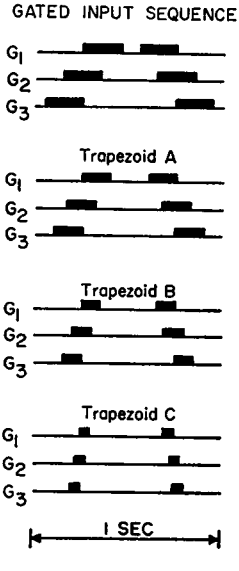


FIGURE 5

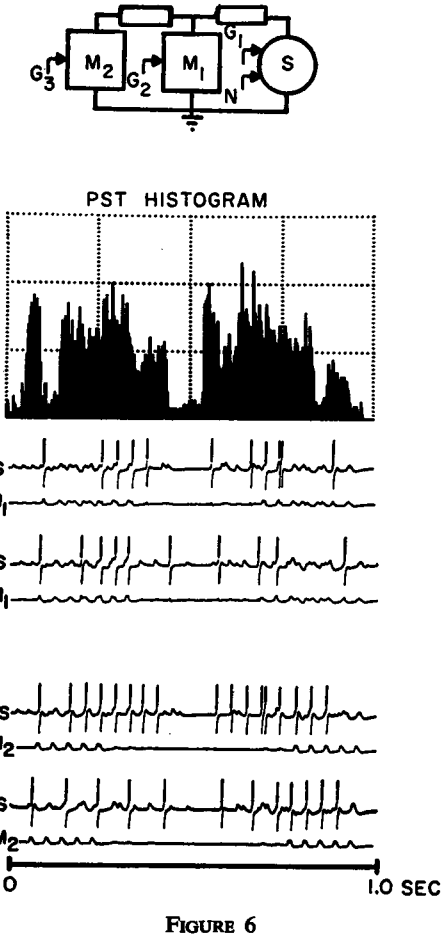


FIGURE 6

FIGURE 5 Temporal conditions for the model stimuli. Each signal line, indicated by a subscripted *G*, is turned on and off according to a programmed pattern. While the signal line is on, a pulse train of fixed frequency is delivered to the synaptic input. (See text.)
FIGURE 6 Typical model configuration and the resulting output. The records indicate membrane potential measured at the spike initiation patch and each subthreshold patch. The signal line (gate) timing is shown in Fig. 5, top. The input labeled *N* is a random (Poisson) noise input.

primary auditory fiber spike trains have been accumulated by Kiang (1965), Rose et al. (1967), and Hind et al. (1967). Since primary auditory fibers provide input spike trains to neurons of the cochlear nucleus, the properties of the input to the simulated cochlear nucleus cells are determined.

For example, the spontaneous activity of auditory fibers has been reported as Poisson in character. Hence the "noise" input to the model may safely be taken as a Poisson process.

For simulating actual auditory stimulation, the gate duration in the model serves to define the length of time during an auditory stimulus that a primary fiber is firing, while the pulse train which is gated approximates the actual primary fiber output. The gate length depends on both the neuron's response area for a given intensity and the auditory stimulus being simulated. Thus, for a tone burst which lies within the response area of a primary fiber, the gate duration lasts the length of the tone burst. For frequency modulation, however, the stimulus "moves through" the response area of the cell and hence the gate should be on during two portions of the stimulus cycle: once as the frequency moves up through the response area, and once as it moves down through the response area. The gate duration depends on both the modeled response area at the given intensity, and the rate of frequency modulation.

Fig. 5 shows a gating sequence which is appropriate for simulating four rates of frequency modulation. As the rate of modulation increases (shown from top to bottom in the figure), the input gate duration is proportionately decreased. This particular set of stimulus gates applies for the examples presented in the following figures where another stimulus set is not shown.

### *Operation of the Model*

The model implicitly has a large number of parameters and hence a still larger number of parameter combinations, each yielding a unique model configuration. One aim of the study was to delimit experimentally this parameter space in order to find the range of values of parameters with which the model best described the observed behavior. The obvious method for working through an experimental problem of this type is to vary systematically a single parameter, holding the remaining parameters constant. Parameters that were varied in this study included simulated cell shape (unipolar, bipolar, etc.), simulated cell size, number and location of synaptic terminations, and the type of input pulse trains.

A single experiment consists of the presentation of 250 stimulus cycles with routine collection of the interval and PST histograms. A stimulus cycle of 1 sec was chosen to coincide with cat cochlear nucleus experiments (the model simulates real time). Fig. 6 indicates a typical spatial configuration, a PST histogram, and membrane potential records. Results reported here are selected from more than 500 such experiments.

## RESULTS AND DISCUSSION

The results are presented in four sections. The first deals with the reproducibility and sensitivity of the model system, the second section with the relationship between the membrane potential and the spike firing pattern for various spatial arrays of the model neuron, the third with the details of modeling the three firing pattern symmetries found in cochlear nucleus neurons, and the fourth with modeling of the constancy of the shape of firing patterns for different modulation rates.

*Reproducibility and General Properties*

Since this simulation was done on analogue devices with digital control, the repeatability or statistical stationarity of the results is important. Stationarity is particularly important since statistical measurements (interval and PST histograms) are used to characterize and assess the behavior of the model. Any drift in parameter values cannot be properly treated. To test the stationarity of the model, identical experiments were performed during the study with the interval between pairs of experiments varying from hours to months. The comparison of spike firing histograms produced by the experiments consistently showed little or no difference (Fernald, 1968).

The general sensitivity of this distributed model to spatiotemporal summation is shown in Fig. 7. The difference between the two cases of Fig. 7 is the sequence of simulated primary fiber center frequencies arrayed along the modeled dendrite. The model cell E-86 has the synapse from its input cell with the highest stimulus frequency most distant from the spike initiator, while the model cell E-90 is the opposite case. There are clear differences between the two cases. First, E-86, with the high frequency input most distant, has approximately 18% more spike firings than E-90. Furthermore, this increase in number of spikes is disproportionately distributed, with more going to the stimulus half-cycle corresponding to the spatiotemporal sweep toward the spike initiator patch. This suggests that the effects of higher excitation at a distance are distributed unequally due to the spatial and temporal summation of the stimulus (in Fig. 7 the values of $f_1$ and $f_3$ differ by 37%). In both case it is important to remember that the same *net* amount of excitation is delivered to the model cell during each half of the stimulus cycle. The difference in

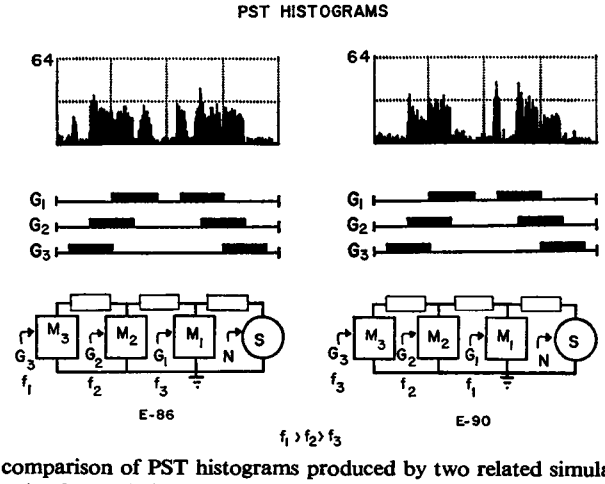


FIGURE 7 A comparison of PST histograms produced by two related simulations. In each case the same stimulus and circuit arrays were used. The gated stimulus pulse frequencies in the two cases are different, however. As illustrated schematically, the frequency of the inputs to $M_1$ and $M_3$ are switched between the two cases, synaptic strength remaining constant.

number of firings and firing pattern between the two halves is entirely a function of the spatial distribution of the inputs. The relative importance of a synaptic input as a function of distance depends greatly on intensity and timing with which it is activated relative to other synaptic inputs on that dendritic branch. It is influenced to a lesser extent by activity on other dendritic branches (cf. Fig. 9 and Fernald, 1968).

*Explicit Simulation of Cochlear Nucleus Data*

*Membrane Potential.* Experimental work in cochlear nucleus neurons (Gerstein et al., 1968; Starr and Britt, 1970) and elsewhere (Spencer and Kandel, 1961) has suggested that the potential measured by the microelectrode in some cases is not simply correlated with generation of spikes. A proposed explanation for such observations is that the electrode is at a point distant from the site of spike initiation, and, at a given moment, that the cell interior is not isopotential. This explanation has been examined with the use of the model, by recording the simulated membrane potential simultaneously at several sites under various stimulus conditions.

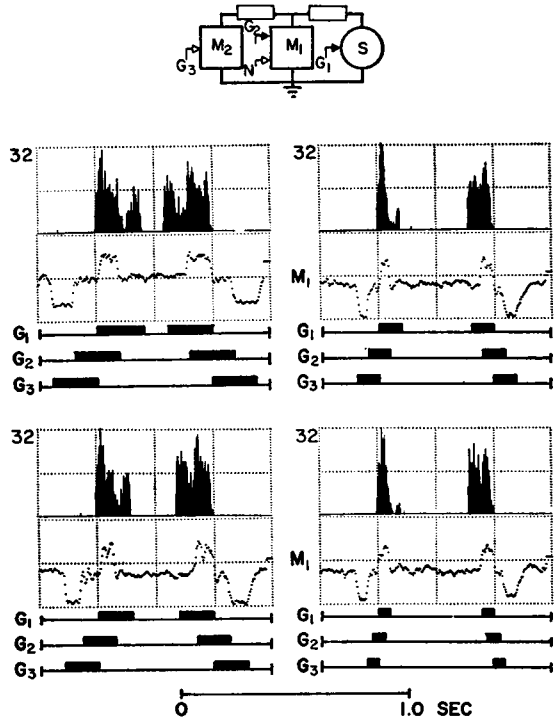


FIGURE 8 PST histograms and averaged membrane potential for a simulation array. The simulation has two inhibitory inputs (indicated by open arrowheads): a gated input to the subthreshold patch $M_2$, and a noise input to subthreshold $M_1$. The remaining inputs are excitatory (indicated by filled arrowheads). The averaged membrane potential measured at the subthreshold patch $M_1$ is shown below each PST histogram.

Fig. 8 shows a family of four simulations at different "stimulus modulation rates." Both the averaged membrane potential from the middle patch and the PST histograms are shown. It is clear that the membrane potential measured at a patch reflects most strongly the synaptic inflow associated with that patch. For the model, predicting the spike firing pattern from the measured membrane potential is more difficult as the point of measurement is increasingly distant from the spike initiator patch. Analogously, we may infer that an electrode which measures the potential some distance from the site of spike initiation in a nerve cell might show little correlation between the behavior of the membrane potential and the form of the output firing pattern.

In some neurons of the cochlear nucleus, the recorded membrane potential depolarized shortly after the onset of the tone burst stimulus, but the spike generation occurred somewhat later (Gerstein et al., 1968). Similar behavior of the model is shown in Fig. 9. The spatial array has excitatory inputs along one equivalent dendritic branch ($M_2$ and $M_3$) and an inhibitory input of the other dendritic branch ($M_1$). In this case the excursions of the averaged membrane potential at subthreshold patch $M_3$ indicate a depolarization unable to influence the firing pattern until released from the inhibitory effects arising on another receptive surface of the cell. Thus, the model shows that the nonuniformity of the membrane potential over the surface of a neuron can account for the lack of correlation between the observed membrane potential and the spike firing pattern.

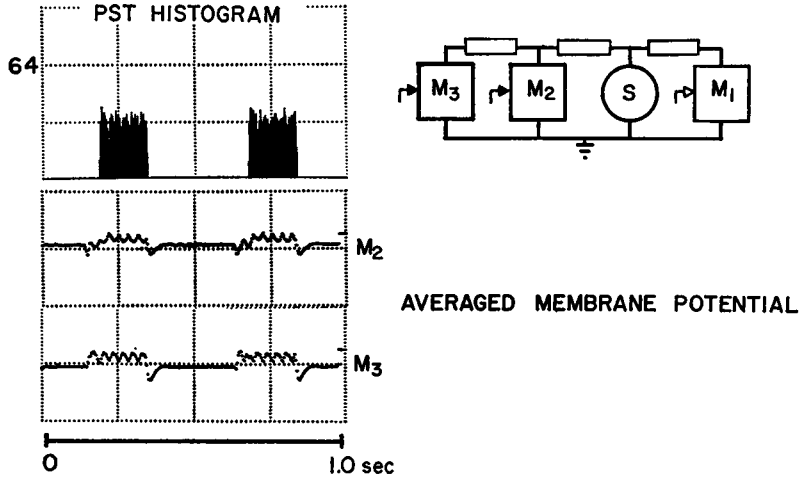


FIGURE 9 PST histogram and two averaged membrane potential measurements for a special configuration of the model. Excitatory inputs are located on one equivalent dendritic branch ($M_2$ and $M_3$) and an inhibitory input located on another dendritic branch ($M_1$). The gated stimulus for the excitatory inputs is that shown in Fig. 5 (top). The gated stimulus for $M_1$ has an identical onset time but only one-fourth the duration. The membrane potential, averaged over 120 stimulus repetitions, is shown for patches $M_2$ and $M_3$.

*Firing Pattern Symmetries*

Cochlear nucleus neurons respond to frequency modulated tonal stimuli with three types of symmetry in the firing pattern (Erulkar et al., 1968, and Fig. 1). The distributed model in an appropriate configuration is able to mimic each of these observed symmetry types. The important model parameters for these properties are spatial arrangement and relative strength of the synaptic input, given a fixed time sequence of synaptic activation. This sequence is chosen to mimic the behavior of primary auditory fibers in response to frequency modulated tones. Fig. 10 shows three model configurations and the corresponding firing patterns. The symmetries shown are relatively insensitive to small changes in the indicated model configurations. Thus each configuration forms a stable, reproducible class of behavior.

*Mirror Symmetry.* A cochlear nucleus neuron having a mirror symmetric firing pattern responds only to the frequency currently being presented, without regard to previous stimulus conditions. That is, the spike response pattern (PST histogram) shows that the cell responds similarly whether its frequency response area is traversed from low to high frequency or from high to low frequency.

In the model there is only one configuration of inputs which consistently yields mirror symmetric response PST histograms. As shown in Fig. 10 *a*, synaptic inputs must be uniformly distributed over the simulated cell input surface. In simulations which give mirror symmetry, spatiotemporal summation is effectively eliminated.

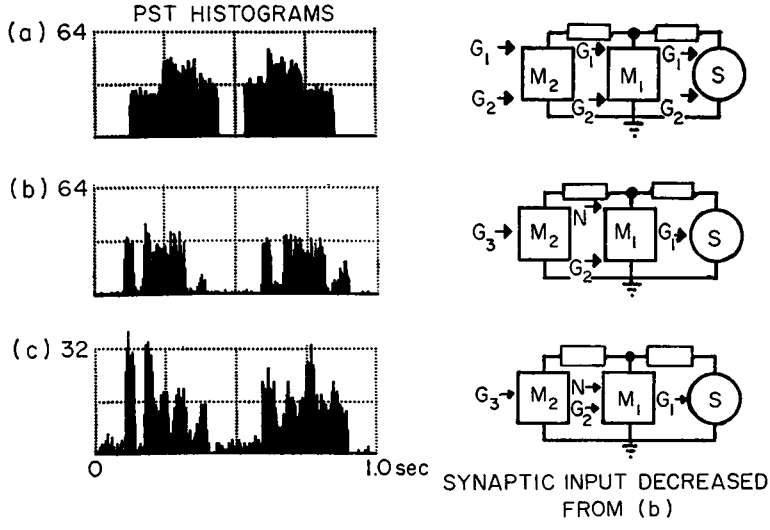


FIGURE 10 PST histograms of firing patterns for three different simulations. The three symmetry classes are: (*a*) mirror symmetry, (*b*) translation symmetry, (*c*) asymmetry. Note that the pertinent difference between asymmetry and translation symmetric neuron models is the intensity of the equivalent synaptic input. Stimulus gates as in Fig. 5 (top).

That is, the synaptic inputs drive the membrane potential uniformly over the whole cell.

This result suggests that cells which produce mirror symmetric firing patterns may receive input fibers uniformly over their surface. Neurons with mirror symmetric firing patterns may be simple follower cells (or relay cells as described by Pfeiffer, 1966) which faithfully respond to the stimulus of the moment.

*Asymmetry.* A cochlear nucleus cell with an asymmetric firing pattern responds to frequency as well as direction and rate of change of frequency. Of these three stimulus properties, an asymmetric cell can detect[2] only the direction of change of frequency. It is important to note that the firing pattern of such a neuron constitutes a "recoding" of the information as it passes through the cochlear nucleus. Information about the the direction and rate of change of frequency are in the spike firing pattern, but changed from the way that they appeared in the stimulus.

As shown previously in Fig. 7, asymmetric firing patterns in the model arise as a consequence of spatiotemporal summation of synaptic inputs over a distributed dendritic surface area. For the firing patterns in Figs. 7 and 10 *c*, the synaptic inputs are sequentially arrayed along a single equivalent dendritic branch. The stimulus sequence moves towards the spike initiator over one half-cycle and reverses that direction over the second half of the stimulus cycle.

*Translation Symmetry.* A cochlear nucleus neuron having a translation symmetric firing pattern responds when the stimulus frequency is within the neuron's response area. The firing pattern gives no indication of detailed frequency or of direction of frequency change. This information is not available to higher neurons since details of the order of frequency presentation do not exist in the firing pattern.

In the model, a range of spatial arrays can produce translation symmetric firing patterns if the intensity of the synaptic input is made sufficiently strong. In this case the simulated cell shows an "onset sensitivity" or exaggerated response to the beginning of the stimulus. This configuration of the model is shown in Figure 10 *b*. The change in symmetry of firing pattern between Figs. 10 *b* and 10 *c* corresponds only to a change in synaptic input strength. In Fig. 10 *b*, subthreshold interactions and spatiotemporal summation at the spike initiator patch are not important in determining the firing pattern.

This modeling result predicts that cochlear nucleus neurons with asymmetric firing patterns will produce translation symmetric firing patterns as the stimulus intensity is increased. Fig. 11, taken from a subsequent physiological experiment, (Fernald and Gerstein, 1970[1]), shows that this is indeed the case. As the stimulus intensity decreases through 20 db, the firing pattern changes from translation to mirror symmetric (Fig. 11 *c*). More generally, this prediction that the translation

[2] I use detection of a stimulus property to mean that the neuron produces a differential response to a change of that stimulus property.

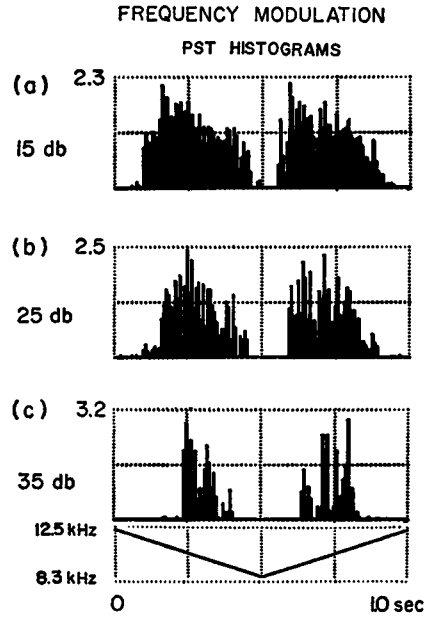


FIGURE 11 PST histograms from a single cochlear nucleus neuron compiled for frequency modulated stimuli at three different intensities. (*a*) most intense stimulus, $S = 28$; (*b*) intermediate, $S = 25$; (*c*) least intense, $S = 20$.

symmetric firing pattern arises from high stimulus intensity might explain the relatively few cases of translation symmetry reported (Erulkar et al., 1968; Fernald and Gerstein, 1970[1]). A more thorough study of firing pattern as a function of stimulus intensity has confirmed the model prediction (Fernald and Gerstein, 1970[1]).

### *Shape Constancy*

In the cochlear nucleus experiments the responses of a single cell to frequency modulated tones were computed for each member of a family of trapezoidal modulation wave forms. For these frequency modulation rates, the spike response pattern shape and symmetry remained constant with a corresponding change in time scale.

Fig. 12 shows a corresponding stimulus set for a simulated nerve cell. Here, too, the shape and symmetry of the spike response histogram is invariant as the effective frequency modulation rate is changed.

Important model constraints on the input are needed for such behavior. In order to simulate different rates of frequency modulation ($df/dt$), only the input gate duration is changed; behavior of an input "fiber" while the gate is open does not change. The input fibers are treated as if there are no lateral interactions.

If similar considerations apply to the physiologically observed shape invariance of the response pattern, then lateral interaction among primary receptors and fibers either does not exist or is constant over the rates of frequency modulation used in the experiments.

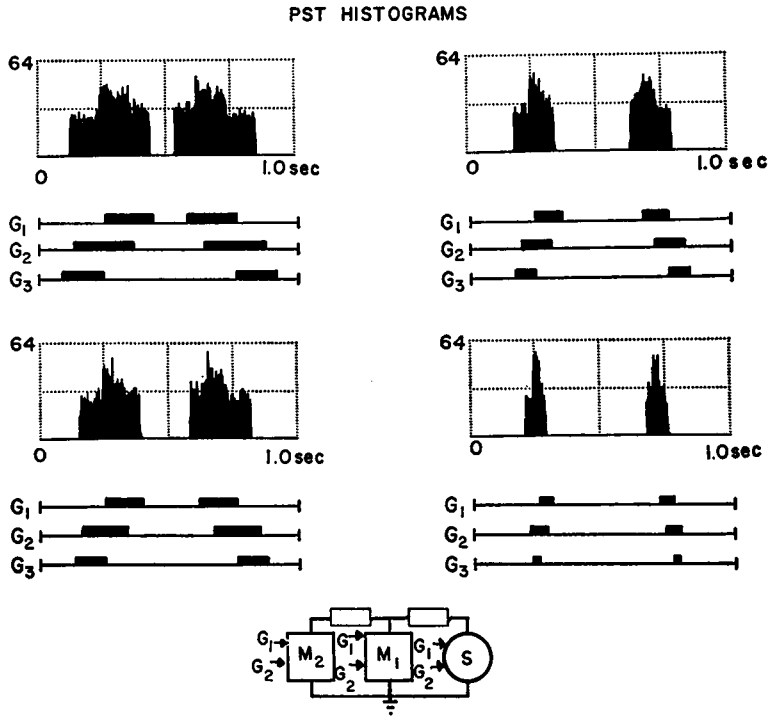


FIGURE 12 A set of four PST histograms from one model in response to the equivalent FM stimulus. Note the constancy of PST histogram shape over the range studied.

## CONCLUSION

Clearly, this neuron model can simulate the important results from the electrophysiological experiments on cat cochlear nucleus neurons. In assessing the validity of this model, several precautions should be noted.

First, the models presented here are not unique since more complex models which produce the same results can be devised. However, available physiological data does not allow sufficient constraints to choose among such models. Several varieties of additional complexity can be envisioned: (*a*) inhibitory inputs, and (*b*) greater complexity of dendritic geometry. I have not systematically examined the effects of inhibitory inputs because the experimental data on IPSP's in cochlear nucleus neurons is difficult to obtain (Gerstein et al., 1968; Starr and Britt, 1970). Nevertheless, it is reasonable to assume that models with inhibitory inputs can also simulate the data (see Fig. 8).

The models presented here have a simple geometry. In the course of this investigation, data were obtained from larger assemblies of simulation circuits. Those results are essentially indistinguishable from the ones presented here.

This study shows that the neuron model can account for a wide range of neural

behavior by virtue of its distributed receptive surface. This suggests that in the physiological system, the synaptic contacts over the dendritic surface area could play an important role in determining single neuron behavior. Spatially arrayed synaptic inputs might generally be important in sensory systems which show a differential response to the direction of change of a dynamic stimulus. The effects of distributed synaptic inputs result directly in such a differential response and might explain similar responses measured for example, in the visual system.

I thank George Gerstein for his helpful comments and discussion throughout the course of the study and during the preparation of the manuscript.
I am extremely grateful to E. R. Lewis for providing the neural patch circuits.
I thank S. Freeman for typing the manuscript and B. Fore for his photographic work.

This study was supported by N.I.H. grants 2-t01-GM-00606 and NB-05606

*Received for publication 29 July 1970 and in revised form 15 December 1970.*

## REFERENCES

ERULKAR, S. D., R. A. BUTLER, and G. L. GERSTEIN. 1968. *J. Neurophysiol.* **31**:537.
FERNALD, R. D. 1967. Proceedings of 20th Conference on Engineering in Medicine and Biology, Boston.
FERNALD, R. D. 1968. Cat cochlear nucleus neurons: a distributed model and some experimental observations. Ph.D. Dissertation. University of Pennsylvania, Philadelphia.
GERSTEIN, G. L., and N. Y-S. KIANG. 1960. *Biophys. J.* **1**:15.
GERSTEIN, G. L., R. A. BUTLER, and S. D. ERULKAR. 1968. *J. Neurophysiol.* **31**:526.
HIND, J. E., D. J. ANDERSON, J. F. BRUGGE, and J. E. ROSE. 1967. *J. Neurophysiol.* **30**:794.
KIANG, N. Y-S. 1965. Discharge Patterns of Single Fibers in the Cat's Auditory Nerve. The M.I.T. Press, Cambridge, Mass.
LEWIS, E. R. 1964. *In* Neural Theory and Modelling. R. F. Reiss, editor. Stanford University Press, Stanford, Calif. 154–189.
LEWIS, E. R. 1965. *J. Theor. Biol.* **10**:125.
LEWIS, E. R. 1968. *Proc. I.E.E.E.* (*Inst. Elec. Electron Eng.*). **56**:931.
LORENTE DE NÓ., R. 1933. *Laryngoscope.* **43**:1.
MOLNAR, C. E., and R. R. PFEIFFER. 1968. *Proc. I.E.E.E.* (*Inst. Elec. Electron Eng.*). **56**:993.
PFEIFFER, R. R. 1966. *Exp. Brain Res.* **1**:220.
RALL, W. 1961/1962. *Ann. N. Y. Acad. Sci.* **96**:1071.
RALL, W. 1964. *In* Neural Theory and Modelling. R. F. Reiss, editor. Stanford University Press, Stanford, Calif. 73–97.
RALL, W., T. G. SMITH, K. FRANK, R. E. BURKE, and P. G. NELSON. 1967. *J. Neurophysiol.* **30**:1169.
RAMON-MOLINER, E. 1962. *J. Comp. Neurol.* **119**:211.
RAMON-MOLINER, E. 1968. *In* The Structure and Function of Nervous Tissue. G. H. Bourne, editor. Academic Press Inc., New York. **1**:205–264.
ROSE, J. E., R. GALAMBOS, and J. R. HUGHES. 1959. *Bull. Johns Hopkins Hosp.* **104**:211.
ROSE, J. E., J. F. BRUGGE, D. J. ANDERSON, and J. E. HIND. 1967. *J. Neurophysiol.* **30**:769.
SPENCER, W. A., and E. R. KANDEL. 1961. *J. Neurophysiol.* **24**:272.
STARR, A., and R. BRITT. 1970. *J. Neurophysiol.* **33**:137.